PERGAMON

Deep-Sea Research II 45 (1998) 1093–1114

DEEP-SEA RESEARCH
PART II

Circulation in the Archipiélago de Colón (Galapagos Islands), November, 1993

John M. Steger[1], Curtis A. Collins*, Peter C. Chu

Department of Oceanography, Naval Postgraduate School, Rm 328, 833 Dyer Road, Monterey, CA 93943, USA

Received 22 October 1995; received in revised form 1 January 1997; accepted 27 January 1997

Abstract

ADCP and CTD data are used to investigate the circulation pattern in the region of the Archipiélago de Colón during the period 8–21 November 1993. Surface flow was dominated by the westward flowing South Equatorial Current except in a small region to the west of Isla Fernandina, where eastward flow associated with the shoaling of the Equatorial Undercurrent was observed. The Equatorial Undercurrent was observed to the west of the Archipelago, centered along 0.5°S at 70 m with peak velocities $\sim 0.6\ m\ s^{-1}$ and, at 92°W, a transport of 6.6 Sv. Between 92°W and the Archipiélago, a distance of only 40 km, the Undercurrent surfaced, the eastward flow decelerated, and meridional flow diverged on either side of 0.5°S, the southward flow appearing to be stronger and better developed than the northward flow. At 89°W the Undercurrent and its associated salinity maximum were observed at 50 m depth at 1°S, with greatly reduced speed, $0.2\ m\ s^{-1}$; subsurface eastward flow also appeared in the northern hemisphere, but this flow was at greater depth, 140 m. The interaction of the Undercurrent and the Archipielago appeared to enhance the thickness of the 16°C thermostad.

1. Introduction

The Archipiélago de Colón (henceforth referred to as the "Archipelago") lays athwart the equator in the Eastern Equatorial Pacific between 89°W and 92°W, stemming and diverting the zonal flows found near the equator (Fig. 1). From the west, the eastward-flowing Equatorial Undercurrent shoals, impinging upon Isla Fernandina and Isla Isabela. From the east, the westward flowing South Equatorial Current sweeps surface waters in and around the Archipelago. The shallow waters of the Archipelago facilitate both the vertical and horizontal mixing of these waters.

* Corresponding author. Tel.: 001 831 656 3271; fax: 001 831 656 3686; e-mail: collins@oc.nps.navy.mil.
[1] Currently at: NOAA Ship RAINIER, 1801 Fairview Ave. East, Seattle, WA 98102, USA.

0967-0645/98/$ – see front matter
PII: S0967-0645(98)00015-0

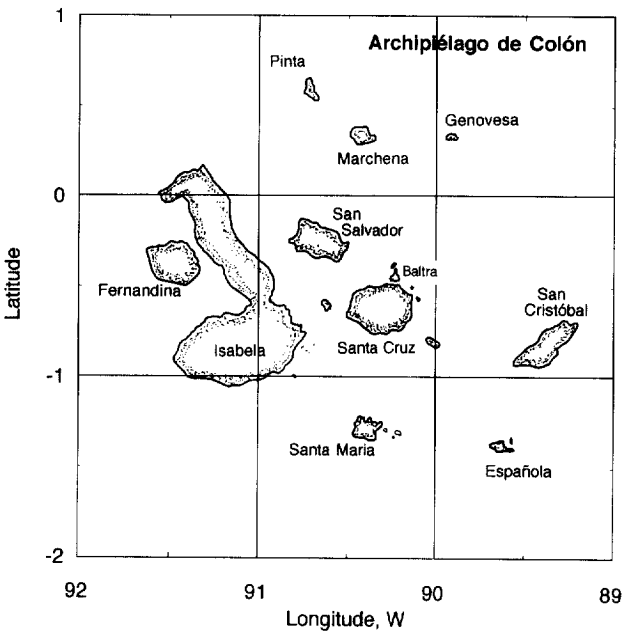

Fig. 1. Chart of the Archipiélago de Colón. Bolivar Channel separates Isla Fernandina and Isla Isabela. Isla Darwin is located at 2°N, 91°W, north of the area depicted on this chart.

Satellite data have shown a biologically rich plume adjacent to and northwest of Islas Fernandina and Isabela (Feldman, 1986). The goal of our measurement program was to measure the circulation around the Archipelago and to try to determine the source waters for this biologically rich plume.

Wyrtki and Kilonsky (1984) provide the canonical description of equatorial circulation in the Central Pacific (150°W–153°W). Features include: (1) an eastward-flowing Equatorial Undercurrent (EUC) extending from 2°S to 2°N, 50–275 m depth, with a transport of 23 Sv and a peak velocity of about 1 $m\,s^{-1}$ occurring on the equator at a depth of 125 m; (2) the South Equatorial Current (SEC) flowing westward above and on either side of the EUC; the flow of the SEC is strongest at the surface, with mean speeds between 0.3 and 0.4 $m\,s^{-1}$; (3) beneath the EUC to about 1000 m, an Equatorial Intermediate Current (EIC) flowing westward intermittently with a maximum mean speed of about 0.1 $m\,s^{-1}$ (Firing, 1987); (4) Subtropical Subsurface Water penetrating the EUC from the Southern Hemisphere with a salinity maximum at the equator of $S = 35.2$; and (5) isotherms diverging above and below the core the EUC indicating upwelling and downwelling, respectively.

These features are modified somewhat near the Archipelago. Knauss (1960) first observed the shoaling of the core of the EUC to 40 m at the Archipelago. During a later cruise, Knauss (1966) tracked the flow of the EUC around the north side of Isla Isabela through a wide and deep gap in the Archipelago between Isla Isabela and Isla Darwin. At 89°W, he observed eastward subsurface flow, but at greater depth

(160–250 m) and reduced velocity (0.1–0.25 m s^{-1}). Christensen (1971) observed the EUC flowing to the north around Isla Isabela in February 1966 and found currents to the south to be weak and irregular. In October and December 1971, Pak and Zaneveld (1973) found that the waters in the EUC to the east of the Archipelago were derived from water flowing around the north side of the islands; they also noted that there was no clear indication of a branch of the EUC to the south of the islands. Wyrtki (1967) used water mass analysis to show that some of the EUC waters recirculate both north and south of the Archipelago. Using historical hydrographic data, Lukas (1986) documented the contribution of eastward-flowing EUC waters to the flow of the Peru-Chile Undercurrent. Lukas (1986) also showed evidence of a seasonal cycle in which the EUC diminishes in the late fall (October to December) at the Archipelago.

More recent observations and modeling of the flows in this region have refined this picture. Leetmaa (1982) showed that the EUC approaches the Archipelago asymmetrically south of the equator and that, as the current decelerates, most of the transport is lost from the upper part of the current. Leetmaa and Wilson (1985) noted that upwelling associated with the divergence of Ekman transport due to northward wind stress occurs south of the equator, between 1°S and 2°S along 85°W, and is confined to the upper 40–50 m. Surface flow is westward at about 0.5 m s^{-1} and, beneath the surface upwelling region, traces of eastward flow occur in and below the pycnocline. Near surface currents are northward and, to the south of the equator, flow in the pycnocline was southward.

2. Measurements

The strategy for the measurement program was to first collect data in the relatively unproductive waters east of the Archipelago along 89°W and then to move to the west of Islas Isabela and Fernandina and locate the plume of high productivity and characterize its horizontal and vertical structure. Sampling was limited by the constraints of available shiptime and chemical reagents. Most data were collected during the period 8–19 November 1993.

Hydrographic data were acquired at 20 stations around the Archipelago (Fig. 2). CTD casts were made to 1500 m or to near the bottom if the water was shallower than 1500 m. Winds, sea surface temperature and sea surface salinity also were monitored continuously using shipboard systems. The processing of the CTD, wind, sea surface temperature and salinity data are described in Miller et al. (1994). Miller et al. (1994) also included descriptions of sea surface conditions.

Currents were observed continuously using a hull-mounted 150 kHz RDI acoustic Doppler current profiler (ADCP). East (u) and north (v) velocity components were averaged in 3 min ensembles in 4 m thick depth bins between 9 and 405 m depth. Data were collected using TRANSECT software (RD Instruments, 1992), and were navigated using GPS data. Several periods of bottom tracking and one course reversal were used to estimate alignment and sensitivity errors following the method of Joyce (1989). Alignment error was $0.31° \pm 0.23°$, and sensitivity error was -0.026 ± 0.005.

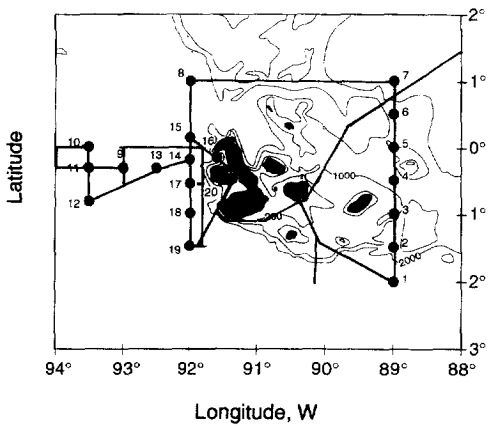

Fig. 2. Cruise track and location of hydrographic stations. 200, 1000 and 2000 m isobaths are shown.

The velocity bin centered on 201 m was used as a reference layer to correct for short-term errors due to GPS and gyro errors (Pollard and Read, 1989). The ADCP data were then manually edited to remove periods when the ship was hove-to (on-station) for extended periods. Finally, gridded fields of 0.01° longitude/latitude were created for each 4 m velocity bin.

Eastward or westward transports were calculated for each bin by multiplying the velocity component by the area of the bin (4423 m^2). Because the north-south sections did not always cover the entire extent of a current regime, total transports could not be estimated. Instead, transport for each current was calculated in 0.25° latitude blocks by summing the bin transports within each current.

Richardson numbers, a measure of the effect of vertically sheared flow on stability, were calculated using CTD and ADCP data. ADCP measurements within 1 km of the CTD station were averaged within each 4 m depth bin. CTD data were used to compute depth and density at 2 dbar intervals. The CTD data were then interpolated to match the depths of the ADCP measurements. At each depth between 9 and 301 m, the Richardson number, Ri, was calculated using the standard formula:

$$\mathrm{Ri} = -\frac{g}{\rho}\frac{\delta\rho/\delta z}{[(\delta u/\delta z)^2 + (\delta v/\delta z)^2]}.$$

Empirical evidence has shown that $\mathrm{Ri} < 0.25$ indicates maintenance or increase of turbulence while larger numbers indicates suppression of turbulence (Pond and Pickard, 1983).

3. El Niño conditions

Because interannual variability plays an important role in determining environmental conditions in the Archipelago, the status of El Niño affects the interpretation

of data from this region. In November 1993, an extended 3 yr El Niño was coming to a close and, although positive sea surface temperatures anomalies greater than 0.5°C dominated the tropics, temperatures in the Archipelago were normal, convection over the central equatorial Pacific was also near normal and the Southern Oscillation Index was near zero (Climate Analysis Center, 1993). Winds measured during the cruise were also consistent with climatology. After removing wind observations collected while the *R/V Iselin* was in port, in Bolivar channel, or in the lee of islands, the vector mean wind speed for the shipboard measurements was 6 m s^{-1}, 166°T. This compares favorably with the November mean winds for the same area from the Hellerman and Rosenstein (1983) climatology of 5 m s^{-1}, 179°T.

Transient equatorial phenomena on time scales shorter than El Niño also could affect our interpretation of the hydrography and currents. Eastward-propagating depressions in the 20°C isotherm (associated with Kelvin waves) originating near 160°W reached the Archipelago (90°W) in May/June 1993 and again in October 1993 and January/February 1994 (Fig. 3a). Hourly detided sea level at Baltra on Santa Cruz Island (Fig. 3b) corroborates this interpretation. Sea levels were elevated April through June and again in October. However, by the period of the cruise (Fig. 3c), sea levels were near-normal (within one standard error of a multi-year biharmonic fit), suggesting that our measurements were minimally affected by transients.

4. Results

Our results are presented as vertical sections of hydrographic properties along 89°W, 92°W, and 0.25°S (Fig. 4), as a series of ADCP sections (Fig. 5), as sections of Richardson numbers (Fig. 6), and as horizontal charts of sea surface conditions (Fig. 7) and currents (Fig. 8). As most of the ocean variability is located in the upper 300 m, only observations to that depth are shown.

5. Vertical sections

89°W. The section along 89°W extended from 2°S to 1°N, passing through the easternmost waters of the Archipelago. Stations were occupied sequentially from south to north, taking almost 3 days to complete the section. Water depths exceeded 1000 m at all stations except at 1°S where our station was 60 km east of Isla San Cristóbal in water 370 m deep. Also note that an unnamed subsurface bank lies just to the east of 89°W at 1.8°S where depth shoals to 200 m.

Surface waters overlay a sharp pycnocline (Fig. 4c, left), located at a depth of about 30 m, which deepened and intensified to the north. Surface salinity at 1°N was about 1 S fresher (Fig. 4b, left) and temperature was 3°C warmer (Fig. 4a, left) than those observed at 2°S, marking the southern edge of the equatorial front. The subsurface salinity maximum (Fig. 4b, left) had $S > 34.95$. Between 1.5°S and 0.5°S, the maximum salinity exceeded $S = 35$ at about 50 m, contrasting with somewhat warmer and

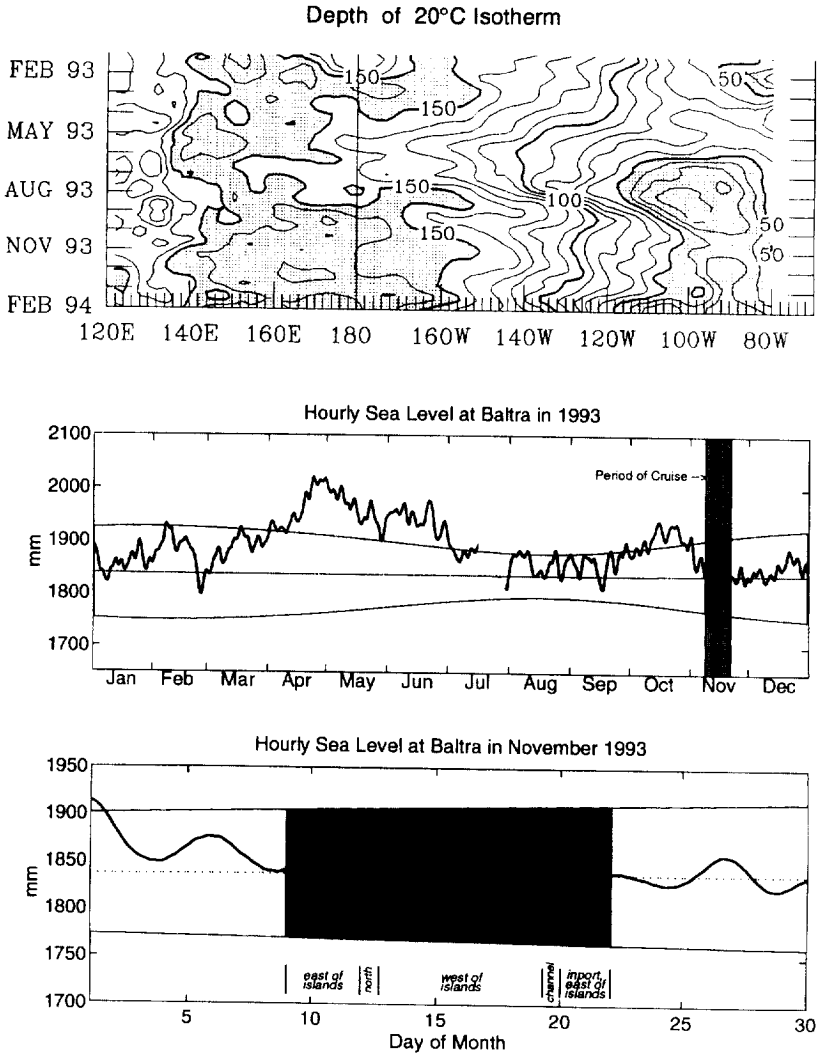

Fig. 3. Variability along the equator in 1993. (upper) Depth of the 20°C isotherm. The contour interval is 10 m with shading for values < 50 m and > 150 m (from figure T16, Climate Analysis Center, 1994). (middle) Hourly sea level at Baltra (Santa Cruz Island) in 1993. The bold line indicates sea level (mm), which has been detided and then low-passed through a 73 h cosine filter. There were data missing in July. The fine line near 1840 mm is a biharmonic least squares fit for annual and semi-annual frequencies using hourly (detided) sea level observed at Baltra between 1985 and 1996; the area within one standard error of the fit is shown by the fine lines above and below. The area of darker shading corresponds to the period of the *R/V Iselin* cruise. (lower) Same as middle except for November 1993. The annotation describes the position of the *R/V Iselin* with respect to the Archipelago.

fresher water at this depth between the equator and 0.5°N. Elsewhere, the salinity maximum was 100 m or deeper, except at 1°N where it was at a depth of 70 m.

The zonal velocity field along 89°W (Fig. 5a) was westward everywhere in the surface layer above the pycnocline. The strongest westward flow, 0.6 m s^{-1}, occurred

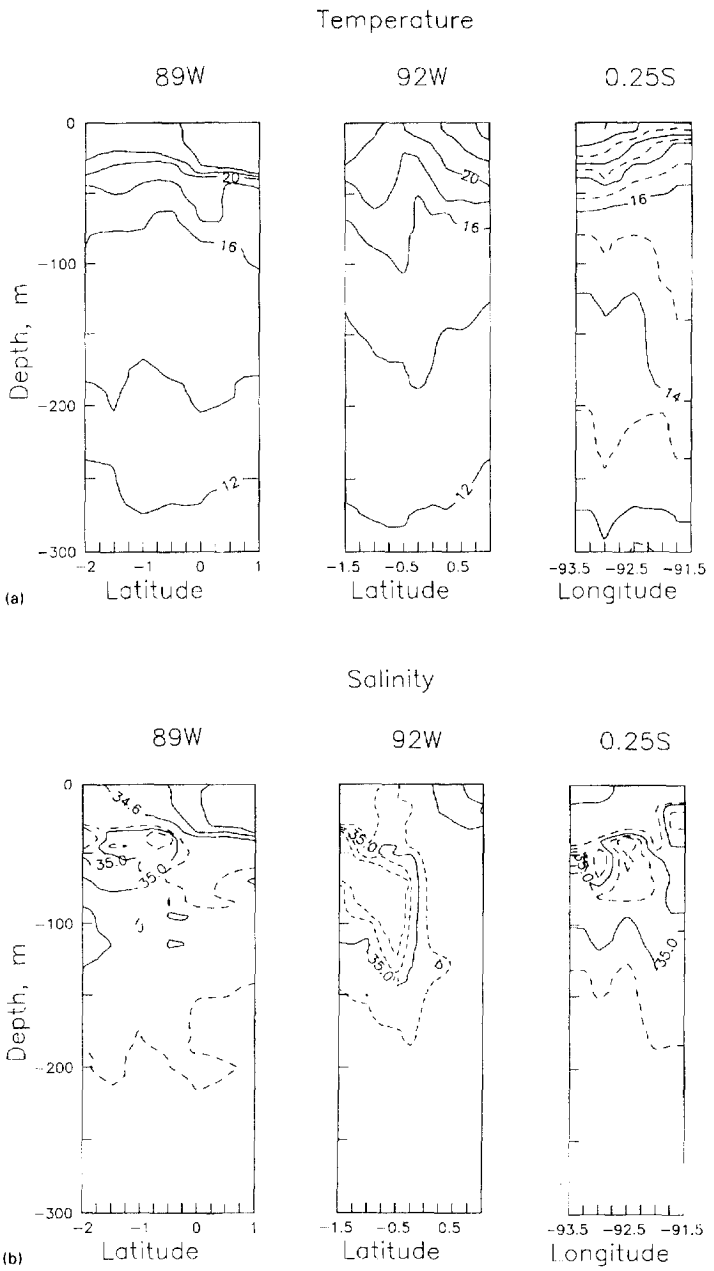

Fig. 4. Hydrography vertical sections at 89°W, 92°W, and 0.25°S. (a) Temperature. The contour interval is 2°C for solid lines and 1°C for dashed lines. (b) Salinity. The contour interval is 0.4 S for solid lines and dashed lines indicate $S = 34.95$, 35.05 and 35.10. (c) Density anomaly. The contour interval is 1 kg m^{-3} for solid lines and dashed lines indicate 25.5, 26.2, 26.4, and 26.6 kg m^{-3}.

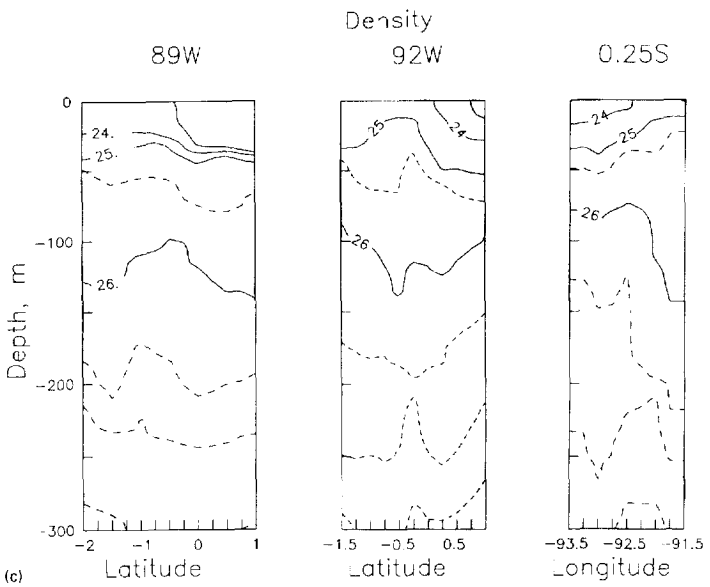

Fig. 4. Continued.

along the frontal zone at 0.4°S where $S = 34.2–33.8$ and 24–25°C surfaced, and which also marked a convergence of the meridional velocity field (Fig. 5a). Two shallow eastward jets were observed: a southern one associated with the shallow (50 m) salinity maximum at 1.4°S, and a northern one at 1°N. The latter also was associated with the subsurface salinity maximum, but at 150 m and somewhat deeper and broader. Both of these eastward flows were marked by a divergence of isotherms associated with eastward flow in the EUC, and had maximum speeds of 0.2–0.3 m s^{-1}. Meridional flow below the pycnocline appeared weak (Fig. 5a). For the subsurface eastward jet to the north of the equator, meridional flow was southward. But for the eastward jet to the south of the equator, meridional flow was northward.

Richardson numbers (Fig. 6) were > 0.25 over most of this section. An active mixing region ($Ri < 0.25$) existed north of the equator near surface ($z < 20$ m).

Nutrients were measured sparsely in the upper ocean waters along 89°W. In surface waters, lowest nutrients were associated with the warmer, fresh waters at the north of the section: nitrates less than 2 μmol kg^{-1}, phosphate less than 0.4 mol kg^{-1}, and silicate less than 1 μmol kg^{-1}. These increased to the south and at 2°S were 8 μmol kg^{-1} nitrate, 0.8 μmol kg^{-1} phosphate and 4 μmol kg^{-1} silicate. Concentrations also increased markedly below the pycnocline.

Fig. 5. ADCP sections at (a) 89°W, (b) 91.75°W, (c) 92°W, (d) 93°W, (e) 93.5°W, (f) 94°W. Zonal velocities are contoured and meridional velocities are indicated by the black arrows. The color bar indicates the magnitude and direction (east or west) for the zonal velocity. The contour interval is 0.2 m s^{-1}. The magnitude of the meridional velocity is given by the arrow in the lower right hand corner of the figure.

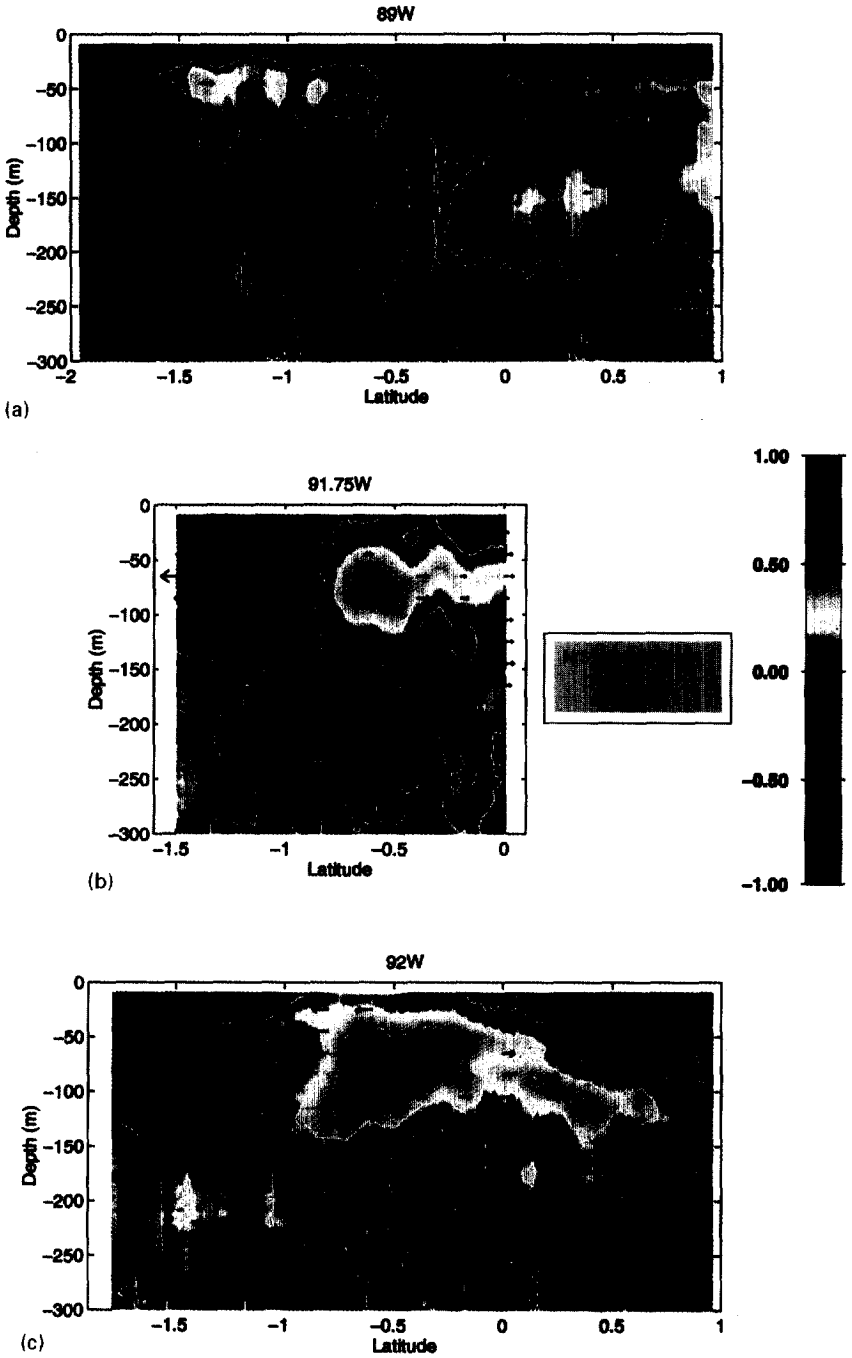
89W
Depth (m)
Latitude
(a)
91.75W
Depth (m)
Latitude
(b)
1.00
0.50
0.00
-0.50
-1.00
92W
Depth (m)
Latitude
(c)

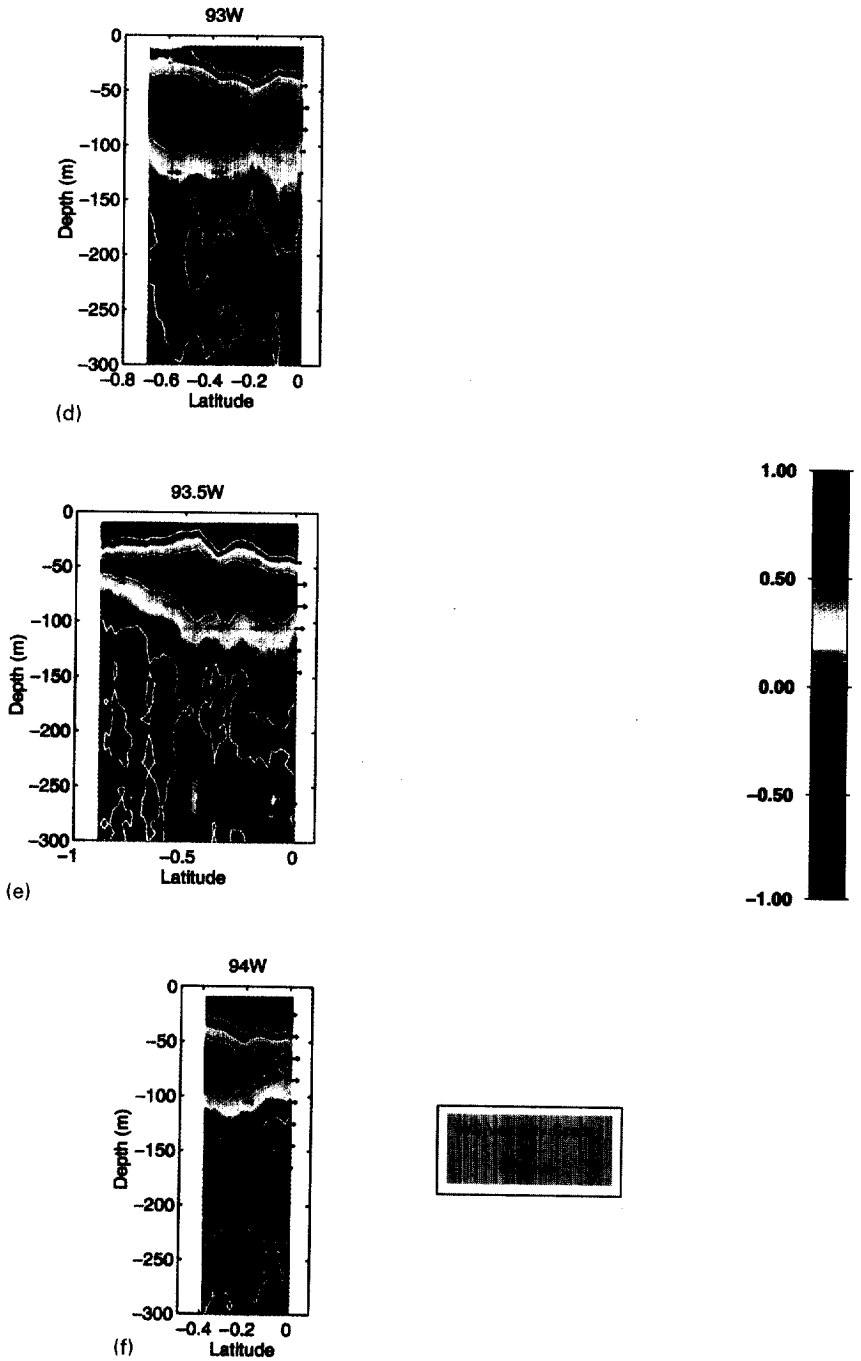

Fig. 5. Continued.

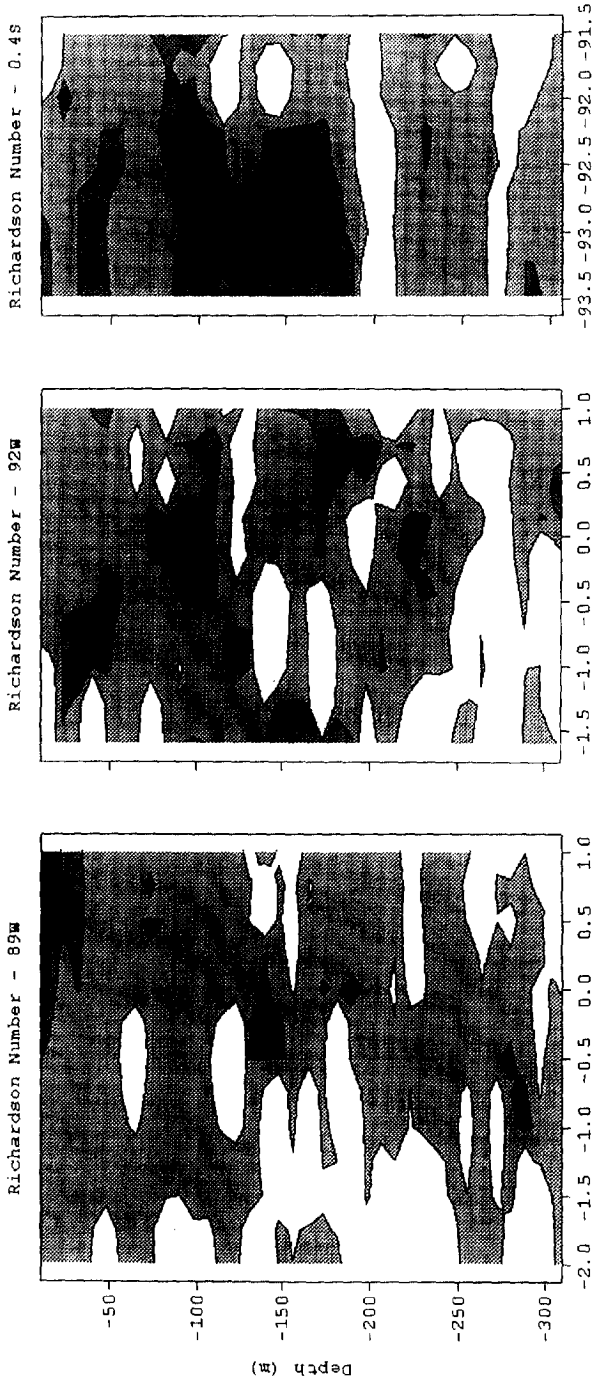

Fig. 6. Vertical sections of Richardson numbers, Ri. Ri > 10 is white, $10 \leqslant \mathrm{Ri} < 1$ is light grey, $1 \leqslant \mathrm{Ri} < 0.25$ is dark grey, and $\mathrm{Ri} \leqslant 0.25$ is black.

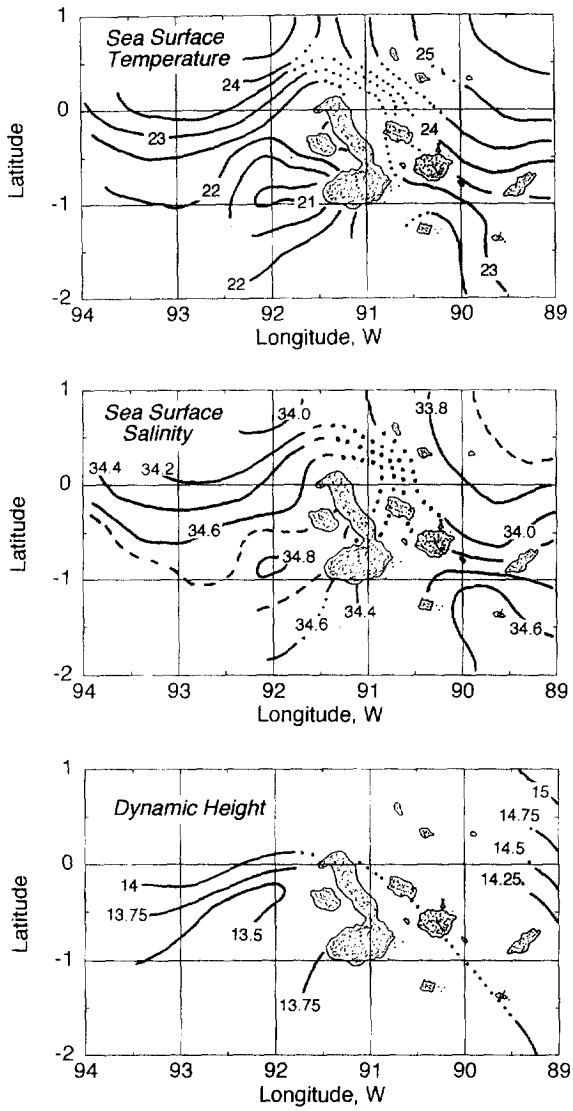

Fig. 7. Sea surface conditions. (upper) Temperature, °C. Contour interval is 0.5°C. Waters in Bolivar Channel to the east of Fernandina are warmer than 22.5°C. (middle) Salinity. Contour interval is $S = 0.2$ except $S = 34.7$ is shown by a dashed line to the west of Isabela and $S = 33.7$ is shown by a dashed line in the northeast corner of the chart. (lower) Dynamic Height ($\Delta D^0/_{1000}$), $m^2 s^{-2}$. Contour interval is 0.25 $m^2 s^{-2}$. Dots are used to connect isopleths in regions with no observations.

91.75°W. The core of the EUC was centered at 0.5°S (Fig. 5b), with maximum eastward velocities of 0.4 m s^{-1} observed between 50 and 100 m depth, 0.4°S and 0.6°S At the surface, weak eastward flow was observed over the core of the EUC. To the north and south of the EUC, the flow was westward. South of the EUC, the westward

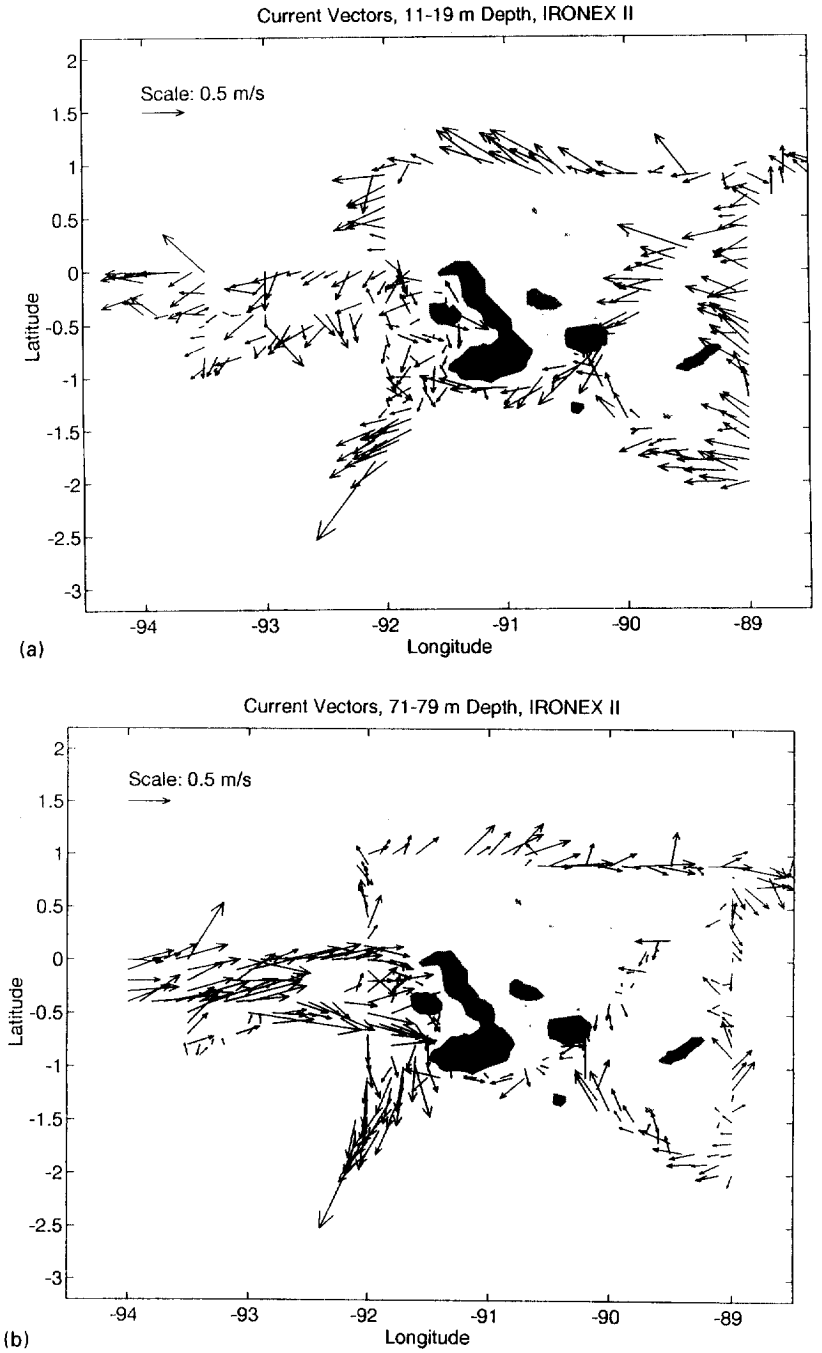

Fig. 8. ADCP velocity vector charts at (a) 15 m, (b) 75 m. Data have been averaged into 0.1° latitude by 0.1° longitude bins. Scale vector shown in upper right.

flow extended from the surface to a depth of 100 m. The meridional flow (Fig. 5b) was weakly sheared and divergent: to the north of 0.5°S the flow was northward, and to the south of 0.5°S the flow was southward, exceeding 1 m s^{-1} at 1.2°S. This maximum southward flow was centered in the pycnocline (not shown), weakening above and below.

92°W. Our sampling sequence along 92°W was not continuous. After reaching the equator, we turned west, surveying the plume area, before returning to occupy hydrographic stations at 0.25°S and 0.25°N on the section. We then occupied a station at the northern end of Bolivar Channel before returning and completing the 92°W section. The southernmost station was completed almost one week after the northernmost station was started.

Along 92°W, the zonal velocity field (Fig. 5c) indicated a much stronger and better developed EUC than the eastward flows observed at either 91.75°W or 89°W. The core of the EUC was marked by velocities exceeding 0.6 m s^{-1} centered at 0.5°S, 80 m deep. Although the subsurface eastward flow extended northward to 1°N, it was neither as thick nor as strong as it was to the south of the equator, possibly due to temporal variability. Strong westward flow was observed in the surface layer, except in the region over the core of the EUC where flow was to the east. The westward flow was best developed to the north of the EUC where a strong jet with velocities exceeding 1 m s^{-1} was observed at 0.5°N, 35 m depth. Beneath the EUC, between 150 and 200 m, weak westward flow was observed.

To the north of the equator above 50 m, the meridional velocity field along 92°W was southward (Fig. 5c). There was a narrow region of northward flow near the equator in this depth zone. To the south, the flow became southward again, with the zero isotach deepening to at least 300 m at 1.5°S. Therefore, with the exception of its southward boundary, most of the EUC appeared to be directed northeastward.

Richardson numbers along 92°W (Fig. 6) were lowest along the base of the EUC between 0.5°S and 0.25°N.

Surface waters were warmest and freshest at 1°N, S = 33.8 and 25.2°C (Fig. 4a and 4b, center panels). A density front occurred in the upper layer in the northern hemisphere, corresponding to a density change of 2 kg m^{-3}, along which strong westward flow was found (Fig. 4c, center panel). This front marked the southern boundary of the Equatorial front (Knauss, 1966). Near-surface upwelling was centered over the EUC between 1°S and 0.5°S, which corresponded to the surface temperature minimum (19.5°C) and salinity maximum ($S = 34.9$) observed along this section. The shallow pycnocline was weaker than that observed at 89°W, especially to the south of the equator. Within and just beneath this shallow pycnocline, a salinity maximum ($S > 35$) extended from the south to 0.25°S, the northern boundary of the strong core of the EUC. At 0.25°S, the isotherm spreading associated with the lower portion of the EUC occurred between 16 and 14°C, while to the north and south the 13°C thermostad dominated.

The nutrient fields all reflect the surface upwelling pattern seen in the temperature, salinity, and density fields. Subsurface, the maximum nutrient concentration at a given level seemed to shift somewhat to the north.

93°W. The core of the EUC was found between 50 and 80 m at 0.5°S. It was marked by eastward velocities exceeding 0.6 m s^{-1} and a northward component of about 0.2 m s^{-1} (Fig. 5d). In and above the pycnocline, the meridional component of flow

appeared convergent at 0.4°S (Fig. 5d), and to the north of this region lay strong westward flow.

A single CTD station was occupied in the middle of this section at 0.4°S (station 9). Salinity maxima ($S = 35.05$) were at 45 and 85 m.

93.5°W. The core of the EUC deepened from 50 m at 1°S to 75 m at the equator (Fig. 5e), with the strongest eastward flow between 0.3°S and 0.5°S. This core had a northward component. Above the EUC, flow was westward, most strongly north of 0.4°S, which corresponded to the convergence of the meridional currents (Fig. 5e). Just to the south of 0.4°S, the meridional components diverged in association with upwelling of isopycnals and isohalines at station 12 (not shown). The $S = 35$ isohaline outlined the eastward flow of the EUC, and $S > 35.2$ was found at the core of the EUC at 1°S.

94°W. The core of the EUC is only partially resolved in this section, and appeared to lie to the south of 0.4°S at a depth of 70 m with maximum velocities exceeding $0.6\,m\,s^{-1}$ (Fig. 5f). Surface flow between the equator and 0.4°S was westward. No hydrographic data were collected along this meridian.

0.25°S. A section was constructed just south of the equator (Fig. 4, right panels). This section consists of stations at 93.5°W, 93°W 92.5°W, 92°W and 91.58°W. The latitude along this section varies somewhat: the first three stations were between 0.35°S and 0.4°S, while the station at 92°W was located at 0.25°S; the easternmost station was located at 0.17°S in water 1700 m deep at the entrance to Bolivar Channel, with Isla Isabela to the north and east and Isla Fernandina to the south. About one week elapsed between the first (station 9) and last (station 16) station along this section.

Hydrographic properties indicated upwelling of isotherms, isohalines and isopycnals in the upper 70 m toward the coast of Isla Isabella. A near-surface salinity maximum was observed at the coast (Fig. 4b, right), and upper waters were stratified below the shallow mixed layer. Beneath the shallow pycnocline (Fig. 4c, right), strong isopycnal downsloping toward the coast was observed to the east of 92.5°W in the depth interval between 70 and 200 m. The 70 m thick 13°C thermostad observed to the west of 92.5°W, shrank to 20–40 m to the east, with corresponding increases in the thickness of the 15°C thermostad, and to a lesser extent, 14°C. The eastward increase in thickness of these waters also was seen in the salinity and density sections.

In the upper waters, nutrients also showed a sharp gradient between 93°W and 93.5°W. Increases were toward the west, consistent with upwelling of these waters. Above 30 m, nitrates increased by $4\,\mu mol\,kg^{-1}$, phosphate by $0.2\,\mu mol\,kg^{-1}$, and silicate by $3\,\mu mol\,kg^{-1}$. Phosphate and nitrate showed no evidence of subsurface deepening toward the coast, although silicate did.

Richardson numbers along this section showed a region of active mixing along the base of the EUC (Fig. 6). The depth of active mixing appeared to shoal from 150 to 75 m at 92°W and thence remained at 75 m at 91.58°W.

6. Spatial variability

Winds were northward over much of the study area, with speeds of about $6\,m\,s^{-1}$ except in the area of Bolivar Channel where winds curved northward around Isla

Fernandina (see Miller et al., 1994, Fig. 2). Surface isotherms and isohalines (Fig. 7) were oriented in a northwest-southeast direction east of the Archipelago, with temperatures decreasing and salinities increasing toward the southwest. Surface waters warmer than 25°C and fresher than $S = 33.7$ lay to the northeast of the Archipelago. To the west, isotherms and isohalines were zonal north of 0.5°S, with temperature increasing and salinity decreasing to the north. Minimum surface temperatures, < 21°C, and maximum salinities, $S > 34.8$, occurred to the west of the southern portion of Isla Isabela.

Dynamic height ($\Delta D^0/_{1000}$) had a similar pattern (Fig. 7), with the largest value, 15.1 $m^2 s^{-2}$, observed at the northeastern extreme of our grid, station 7. The lowest value, 13.3 $m^2 s^{-2}$, occurred just to the west of Isla Fernandina at station 14. A trough of low dynamic height, $\Delta D^0/_{1000} < 13.6\ m^2 s^{-2}$, extended from the west–southwest and included stations 12, 13 and 14. Dynamic heights were greater at 89°W than 92°W (0.5 $m^2 s^{-2}$ on average), and this difference was three times greater north of 0.5°S than to the south.

Current charts were constructed by binning ADCP observations into boxes 0.1° square and averaging. Current charts are shown for surface currents (15 m) and for the EUC (75 m).

Surface (15 m). Surface currents (Fig. 8a) were westward at most locations with typical speeds of 0.5 $m s^{-1}$. South of the Archipelago, currents were directed strongly to the west, but appeared to be deflected southward and southwestward when they reached 92°W. Surface currents east of the islands were directed to the northwest along the 1000 m isobath and through a channel between Isla Genovesa (located at 0.3°N, 89.9°W) and a subsurface bank, although currents observed along 1°N also had a northward component, possibly due to southerly winds. Surface currents west of the Archipelago were typically weaker and to the southwest. Some eastward flow was observed to the south and west of Isla Fernandina. The region of strongest flow was located southwest of Isla Isabela where currents flowed to the southwest.

EUC (75 m). Flow at this depth was dominated by the EUC (Fig. 8a). West of the Archipelago, speeds typically exceeded 0.5 $m s^{-1}$ to the east. These eastward flows had a northward component north of 0.5°S, but south of this latitude they were directed southward. Southwest of Isla Fernandina, the strong and coherent flow was directed somewhat more to the south than that observed at the surface. At this depth, a weaker eastward flow was observed along 1°N. Flow at this depth does not represent the core of the EUC to the east of the Archipelago because the core of the EUC lay above 75 m to the south of 0.5°S and at 150 m to the north of the equator (Fig. 5a).

A strong meridional divergence occurred in the southwest corner of the Archipelago in both the surface currents (Fig. 8a) and EUC (Fig. 8a). This must be due to the zonal convergence as the EUC impacts the Galapagos.

7. Tidal variability in Bolivar Channel

Upper ocean waters within the Archipelago tend to be better mixed than those in the open ocean due to their interaction with topography. A variety of processes,

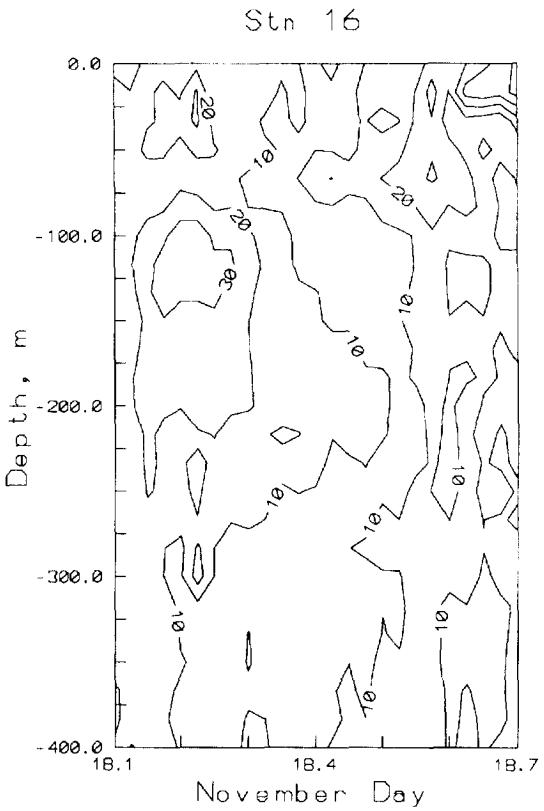

Fig. 9. ADCP speed at the northern entrance to Bolivar Channel (Station 16, Fig. 2). The contour interval is 0.1 $m\,s^{-1}$.

including tides and island wakes, contribute to this mixing. Feldman (1986) suggested that the large area of high productivity occasionally seen to the west of the Archipelago occurs during periods when mixing processes within the Archipelago supply nutrients to the larger plume via enhanced westward transport by the SEC.

To get an estimate of the degree of mixing associated with tidal currents, ADCP data collected at a single station in water 1.7 km deep at the entrance to Bolivar Channel (station 16, Fig. 2) were examined. This station was located in an area of maximum surface productivity in October 1983 (Fig. 1a, Martin et al., 1994). These ADCP data were processed as described above, then averaged every 6 min.

The tidal regime in the Archipelago is "semidiurnal", and the amplitude of the semidiurnal principal lunar (M_2) tide is 65 cm at Santa Cruz Island. The M_2 amphidrome is located about 1000 km west of the Archipelago, with a cotidal line extending eastward to the coast of South America through the islands (Schwiderski, 1983). The M_2 tide moves clockwise about this amphidrome, with amplitude increasing into the Gulf of Panama.

The flow at station 16 had a semidiurnal character (Fig. 9). Flows were strongest, 0.3 $m\,s^{-1}$, at 0445 and 1645; the former was clearly resolved as a subsurface maximum

at 125 m while the latter appeared at the surface and was increasing at the end of the record. The stratification was similar at each of the two CTD casts made at this location, with a maximum gradient of 0.25 $kg\,m^{-4}$ at a depth of 10 m. Velocity data obtained during passage through Bolivar Channel and at Station 20 were similar to the flow patterns seen at station 16. The stratification at Station 20 was also similar to that at station 16, 0.25 $kg\,m^{-4}$ at a depths of 10–20 m.

Simpson and Hunter (1974) showed that the water column becomes homogeneous when the ratio of the bottom depth (in meters) to the cube of the amplitude of the tidal flow (in meters per second) is near a critical value of 55 ($s^3\,m^{-2}$). Using this relationship, the tidal currents we observed in and near the Bolivar Channel would effectively mix the entire water column only where the water is a few meters deep. This suggests that tidal mixing of the sort that may bring nutrients to the surface is constrained to the nearshore of the Archipelago.

8. Discussion

The surface circulation was dominated by westward flow associated with the SEC. To the east and north of the Archipelago, this westward flow had a northward component that appeared to be strongest along the edge of the equatorial front (which marked the boundary of waters of $\gamma < 23\,kg\,m^{-3}$, temperature $> 24°C$, and $S < 34.4$ which lay to the northeast). The surface flow was westward south of the Archipelago. West of the Archipelago, the westward flow had a southward component. Eastward flow associated with the surfacing of the EUC can be seen in the region immediately to the west of Isla Fernandina. Finally, southwest of Isla Isabela the surface flow is directed to the southwest with speeds $\sim 1\,m\,s^{-1}$.

Although historical hydrographic data suggest that the Undercurrent is not present immediately to the west of the Galapagos in November (Lukas, 1986), we observed a region of strong, well-developed eastward flow. Highest velocities in the EUC were observed at 70 m, and the core appeared to be centered at 0.5°S in the sections to the west of the Archipelago. This eastward transport was centered just below the 16°C isotherm, and its southern half was marked by $S > 35$. Immediately to the west of the Archipelago, the EUC transport south of 0.5°S turns southward. The southward flow at the southern boundary of the Archipelago intensified and deflected to the southwest. The eastward transport of the EUC was 6.6 Sv at 92°W, but decreased to only 2 Sv at 91.75°W. At 89°W, the character of eastward flow changed dramatically, and two weak cores were observed: at 50 m, between 1.5°S and 1°S and at 150 m between the equator and 1°N. The transport of the former was 0.7 Sv while the latter was 2 Sv, with probably more eastward flow to the north of our section (on November 21, while returning to the Canal Zone, we observed this branch of the EUC to be located between 0.36°N, 89.5°W and 1°N, 88.7°W at 100 m depth and transport of 0.8 Sv). The southern core of eastward flow was connected with the EUC west of the Archipelago but at depths intermediate between those depicted in Fig. 5a and b; the salinity and temperature of these waters were similar to that of the EUC. It is also interesting that at 89°W the eastward flow in the southern hemisphere had a northward component

while in the northern hemisphere it had a southward component, indicating the possibility that the two eastward flows join further to the east.

The blocking of eastward transport of 16°C water by the Archipelago builds a deep thermostad of these waters at 91.5°W. The 13°C thermostad appeared to be of normal thickness (75 m) and depth (200 m) (see Lukas, 1986, Fig. 6) at 93°W, but was greatly reduced in thickness at 91.5°W where the 16°C thermostad was increased. Above 70 m, temperature, salinity, and density gradients are sloped sharply toward the surface as the Archipelago is approached along 0.25°S. Along 92°W, this upwelling appeared to occur to the north of 0.7°S at the surface, and the upwelling zone shifted north to 0.25°S at 75–100 m depth.

Despite this upwelling, the temperature of the upper ocean appeared to be unseasonally warm on the equator at 92°W compared with historical hydrographic data (Lukas, 1986) even though El Niño conditions appeared near normal (Climate Analysis Center, 1993). At 50 m, observed temperatures were 17.3°C and salinity was 34.94 vice 14.3°C and 34.96 for historical data (Lukas, 1986, Fig. 12).

As noted in the Introduction, the westward flow beneath the EUC is called the EIC. This flow was best resolved by our sections at 91.75°W and 92°W. At both meridians, the EIC appeared centered at a depth of 200 m at 0.5°S with a speed of 0.1–0.2 $m\,s^{-1}$. Corresponding transports were 0.3 and 0.4 Sv. At 93°W, the EIC was somewhat deeper, 220 m, and displaced northward to 0.3°S. At 93.5°W, the eastward flow associated with the EIC was disorganized, while at 94°W it appeared between 150 and 250 m across the short section. Along 89°W, flow was westward beneath both the southern and northern EUC.

The deceleration of the eastward flow in the EUC took place within 30 km of the coast of Isla Fernandina. Flow at 92°W was qualitatively similar to that observed along meridians at 93°W, 93.5°W, and 94°W, but at 91.75°W the eastward transport was less than a third of that observed at 92°W. The westward pressure gradients (calculated with respect to 1500 db) west of station 14 reversed between stations 14 and 16. This eastward pressure gradient was zero at 750 m, and increased linearly with decreasing pressure to a maximum of $10^{-6}\,m\,s^{-2}$ at a depth of 50 m. For these two stations, we evaluated three terms of the zonal momentum balance: the zonal advection of zonal momentum, $\bar{u}(\delta u/\delta z)$; the vertical advection of eastward momentum, $\bar{w}(\delta u/\delta z)$ ($\bar{w}$ was estimated as the product of u and the isopycnal slopes between the stations); and the zonal pressure gradient, $(1/\rho)(\delta\bar{p}/\delta x)$. The momentum advection terms fail to balance the pressure gradient by a factor of five, but errors in the estimate of the advection terms (due to the fact that the measurements were not made at the same time) were of the same order of magnitude as the zonal pressure gradient. Therefore, it is not possible to make any conclusions regarding the importance of turbulent fluxes and local acceleration in this regime.

As pointed out by Hayes (1985), the sea level difference across the Archipelago should increase as the strength of the EUC increases. Using sea-level differences between Isla Isabela and Isla San Cristobal and current measurements from the equator, 95°W, Hayes showed $u|u| \approx \Delta p/\rho$. If we use the maximum isotach from Fig. 5c at 0.5°S, ($0.6\,m\,s^{-1}$), then $u|u|$ is $0.36\,m^2\,s^{-2}$ and the mean difference of

dynamic height between 89°W and 92°W across this latitude zone was 0.42 $m^2 s^{-2}$. This agrees well with Hayes's result.

The strong southward flow just southwest of the Archipelago has not been previously reported. We have looked at sea-level variability, and see no evidence of Kelvin wave activity or rapid change in sea level during the period of our observations (Fig. 3). Lukas (1986, Fig. 14) reported an oxygen maximum at 100 m (associated with Undercurrent waters) extending from the equator toward the south in this region. This pattern is consistent with the velocity field that we observed.

We also saw clear differences in the EUC to the north and the south of the Archipelago. Although the velocities were reduced to $\sim 0.2\ m\ s^{-1}$ to the south, the EUC was shallow (above 50 m), while to the north it was at a depth of 150 m. (The latter feature also was clearly documented by Knauss, 1966). This might be caused by the horizontal divergence (convergence) to the south (north) of the Archipelago.

Finally, we address the question of the source of the biologically rich plume. It is clear that the near-surface waters that lay to the west of the Archipelago during November 1993 were largely derived from the EUC, and as a consequence were cooler and saltier with higher concentrations of nutrients and iron than waters found to the east of the Archipelago. The areal extent of the plume shown by Feldman (1986) and observed during our cruise was too great to be sustained by tidal mixing processes given the observed speeds of surface currents and the rate of consumption of nutrients and iron by phytoplankton. We predict that this will be confirmed by SeaWIFS observations; i.e., that when there is no EUC in the region of the Archipelago, the biological activity will be absent.

Acknowledgements

Our participation in this program was largely due to the efforts of John Martin and Tim Stanton. Cruise participation was supported by the Office of Naval Research and benefitted from the able assistance of Vernon Anderson. Sea level data and associated tidal analyses were supplied by the University of Hawaii Sea Level Center. Data analysis and interpretation has been supported by the Naval Postgraduate School and the Pacific Fisheries Environmental Group of the National Oceanic and Atmospheric Administration. The manuscript was greatly improved by the helpful suggestions of Frank Schwing, Leslie Rosenfeld, Toby Garfield, and two anonymous referees.

References

Christensen, N., 1971. Observations of the cromwell current near the Galapagos Islands. Deep-sea research 18, 27–33.

Climate Analysis Center, 1993. Climate Diagnostics Bulletin, November, 1993. NOAA, U.S. Department of Commerce, 74 pp.

Climate Analysis Center, 1994. Climate Diagnostics Bulletin, February, 1994. NOAA, U.S. Department of Commerce, 80 pp.

Feldman, G.C., 1986. Patterns of the phytoplankton production around the Galapagos Islands. In: J. Brown, Yentsch, M., Peterson, W.T. (Eds.), Tidal Mixing and Plankton Dynamics: Notes on Coastal and Estuarine Studies, Springer, Berlin, pp. 77–106.

Firing, E., 1987. Deep zonal currents in the central equatorial Pacific. Journal of Marine Research 45(4) 791–812.

Hayes, S.P., Mangum, L.J., Barber, R.T., Huyer, A., Smith, R.L., 1986. Hydrographic Variability West of the Galapagos Islands during the 1982–93 El Niño, Progress in Oceanography 17, 137–162.

Hayes, S.P., 1985. Sea level and near surface temperature variability at the Galápagos Islands, 1979–1983. In: Robinson, G., Del Pino, E. (Eds.), El Niño in the Galápagos Islands: The 1981–1983 Event. Charles Darwin Foundation for the Galápagos Islands, Quito, pp. 49–81.

Hellerman, S., Rosenstein, M., 1983. Normal monthly wind stress over the world ocean with error estimates, Journal of Physical Oceanography 13, 1093–1104.

Joyce, T.M., 1989. On *in situ* calibration of shipboard ADCPs. Journal of Atmospheric Oceanography Technology 6, 169–172.

Knauss, J.A., 1960. Measurements of the Cromwell Current. Deep-Sea Research 6(4), 265–285.

Knauss, J.A., 1966. Further measurements and observations on the Cromwell Current. Journal of Marine Research 24(2), 205–240.

Leetmaa, A., 1982. Observations of near-equatorial flows in the eastern Pacific. Journal of Marine Research 40 (supplement), 357–370.

Leetmaa, A., Wilson, D., 1985. Characteristics of near surface circulation patterns in the eastern equatorial Pacific, Progress in Oceanography 14, 339–352.

Lukas, R., 1986. The termination of the Equatorial Undercurrent in the Eastern Pacific, Progress in Oceanography (16), 63–90.

Martin, J.H., Coale, K.H., Johnson, K.S., Fitzwater, S.E., Gordon, R.M., Tanner, S.J., Hunter, C.N., Elrod, V.A., Coley, J.L., Barber, R.T., Lindley, S., Watson, A.J., Van Scoy, K., Law, C.S., Liddicoat, M.I., Ling, R., Stanton, T., Stockel, J., Collins, C., Anderson, A., Bidigare, R., Ondrusek, M., Latasa, M., Millero, F.J., Lee, K., Yao, W., Zhang, J.Z., Friederich, G., Sakamoto, C., Chavez, F., Buck, K., Kolber, Z., Greene, R., Falkowski, P., Chisholm, S.W., Hoge, F., Swift, R., Yungel, J., Turner, S., Nightingale, P., Hatton, A., Liss, P., Tindale, N.W., 1994. Testing the iron hypothesis in ecosystems of the equatorial Pacific Ocean. Nature 371, 123–129.

Miller, B.H., Anderson, V.N., Collins, C.A., 1994. Hydrographic data from equatorial Pacific waters near the Galapagos, November 1993. NPS Technical Report NPS-OC-94-002, Naval Postgraduate School, Monterey, CA, 54 pp.

Pak, H., Zaneveld, J.R.V., 1973. The Cromwell Current on the East Side of the Galapagos Islands. Journal of Geophysical Research 78, 7845–7859.

Pollard, R., Read, J., 1989. A method for calibrating shipmounted acoustic Doppler profilers and the limitations of gyro compasses. Journal of Atmospheric Oceanographic Technology 6, 859–865.

Pond, S., Pickard, G.L., 1983. Introductory Dynamical Oceanography, 2nd ed. Pergamon Press, Oxford, 329 pp.

Instruments, R.D., 1992. TRANSECT Users Manual for Narrow Band ADCPs, R. D. Instruments, San Diego, CA.

Schwiderski, E.W., 1983. Atlas of Ocean Tidal Charts and Maps, Part I: The Semidiurnal Principal Lunar Tide M2. Marine Geodesy 6(3–4), 219–265.

Simpson, J.H., Hunter, J.R., 1974. Fronts in the Irish Sea. Nature 250, 404–406.
Wyrtki, K., 1966. Circulation and water masses in the eastern equatorial Pacific Ocean. Internaional Journal of Oceanology and Limnology 1(2), 117–147.
Wyrtki, K., Kilonsky, B., 1984. Mean water and current structure during the Hawaii-to-Tahiti Shuttle Experiment. Journal of Physical Oceanography 14, 242–254.